

## Numerical solution of axisymmetric stagnation flow of Newtonian fluid towards a shrinking sheet by SOR iterative procedure

*Mohammad Shafique<sup>1</sup>, Atif Nazir<sup>2</sup>, and Sajjad Hussain<sup>3</sup>*

<sup>1</sup>Ex-AP, Department of Mathematics,  
Gomal University,  
D I Khan, Pakistan

<sup>2</sup>Mathematics Group Coordinator,  
Yanbu Industrial College,  
Yanbu, Saudi Arabia

<sup>3</sup>Department of Mathematics,  
College of Science,  
Al-Zulfi, Saudi Arabia

---

Copyright © 2015 ISSR Journals. This is an open access article distributed under the *Creative Commons Attribution License*, which permits unrestricted use, distribution, and reproduction in any medium, provided the original work is properly cited.

**ABSTRACT:** The axisymmetric stagnation flows towards a shrinking sheet of Newtonian fluids has been solved numerically by using SOR Iterative Procedure. The similarity transformations have been used to reduce the highly nonlinear partial differential equations to ordinary differential equations. The results have been calculated on three different grid sizes to check the accuracy of the results. The problem relates to the axisymmetric stagnation flows towards a shrinking sheet when  $\alpha < 0$  and if  $\alpha > 0$  the axisymmetric stagnation flows towards a stretching sheet. The numerical results for Newtonian fluids are found in good agreement with those obtained previously.

**KEYWORDS:** Newtonian fluids, Shrinking Sheet and SOR Iterative Procedure.

### 1 INTRODUCTION

The problem of fluid flow near a stagnation point has been investigated in numerous ways including porous medium, MHD flow, heat transfer and stretching surfaces. The results of these studies have great practical importance in the prediction of skin friction, heat and mass transfer in high speed flows, drag reduction, transpiration cooling and designing of thrust bearings and radial diffuser. However, in recent years, the problem of stagnation flows about shrinking sheet has attracted the attention of some researchers including Wang [1] studied the stagnation flow towards a shrinking sheet. Fang and Zhang [2] considered MHD flow over a shrinking sheet and obtained closed form exact solution for the problem. The MHD boundary layer flow of fluid over a shrinking sheet has been studied by Hayat et al [3] and Fang [4]. Nadeem et al [5] and Ara et al [6] have been investigated MHD boundary layer flow of fluid over an exponentially permeable shrinking sheet. The steady boundary layer flow and steady two-dimensional flow of a nanofluid past a nonlinearly permeable stretching/shrinking sheet is numerically studied by Zaimi et al [7, 8]. Sajid and Hayat [9] applied homotopy analysis method for MHD viscous flow due to a shrinking sheet. The problem of [9] is studied by Noor et al. [10] by using simple non-perturbative method.

Wang [1], he found the results for the range  $-1 \leq \alpha \leq 5.0$  and concluded, no solution exists for  $\alpha < -1$ . We intend to give an extension to this problem for the range  $-1.1 \leq \alpha \leq 10$ . This particular range of parameter  $\alpha$  has been taken in view of convergence of our numerical scheme. We concluded that the solution exists in the extended range of parameter  $\alpha$ . This

shows that our numerical scheme is better than that of Wang [1]. The governing partial differential equations are reduced to ordinary differential form by using similarity transformation. The resulting equations are then solved numerically by using SOR method and Simpson's (1/3) rule with the formula of Adams-Moulton. The numerical solutions are computed for several values of the parameter  $\alpha$  and the Prandtl number Pr. When  $\alpha \geq 0$ , the flow is towards a stretching disk. When  $\alpha < 0$ , the flow is towards a shrinking sheet.

## 2 MATHEMATICAL ANALYSIS

The steady, incompressible and axisymmetric fluid flow has been analyzed. The flow is in the frame of Cartesian coordinates. The velocity vector is represented by  $\underline{V} = V(u, v, w)$ . The stagnation flow at infinity is given by  $u = ax, w = -az$  where  $a$  is the strength of the stagnation flow. The velocity components, on the stretching surface are  $u = b(x + c), w = 0$ , where  $b$  is stretching rate and  $b < 0$  indicates the shrinking of the surface. The stretching origin is located at  $-c$ . The distance between the axis of the stagnation flow and the center of the shrinking surface is  $c$ . The body force is neglected.

The continuity equation and the Navier-Stokes equations for the flow yield a set of partial differential equations by using the following these assumptions, become:

$$\frac{\partial u}{\partial x} + \frac{\partial v}{\partial y} + \frac{\partial w}{\partial z} = 0, \tag{1}$$

$$v \left( \frac{\partial^2 u}{\partial x^2} + \frac{\partial^2 u}{\partial y^2} + \frac{\partial^2 u}{\partial z^2} \right) - \frac{1}{\rho} \frac{\partial \pi}{\partial x} = u \frac{\partial u}{\partial x} + v \frac{\partial u}{\partial y} + w \frac{\partial u}{\partial z}, \tag{2}$$

$$v \left( \frac{\partial^2 v}{\partial x^2} + \frac{\partial^2 v}{\partial y^2} + \frac{\partial^2 v}{\partial z^2} \right) - \frac{1}{\rho} \frac{\partial \pi}{\partial y} = u \frac{\partial v}{\partial x} + v \frac{\partial v}{\partial y} + w \frac{\partial v}{\partial z}, \tag{3}$$

$$v \left( \frac{\partial^2 w}{\partial x^2} + \frac{\partial^2 w}{\partial y^2} + \frac{\partial^2 w}{\partial z^2} \right) - \frac{1}{\rho} \frac{\partial \pi}{\partial z} = u \frac{\partial w}{\partial x} + v \frac{\partial w}{\partial y} + w \frac{\partial w}{\partial z}, \tag{4}$$

$$\rho C_p \left( u \frac{\partial T}{\partial x} + v \frac{\partial T}{\partial y} + w \frac{\partial T}{\partial z} \right) = K \left( \frac{\partial^2 T}{\partial x^2} + \frac{\partial^2 T}{\partial y^2} + \frac{\partial^2 T}{\partial z^2} \right). \tag{5}$$

The following similarity transformations are used to convert the governing partial differential equations into ordinary differential form.

$$\begin{cases} u = axf'(\eta) + bcg(\eta), v = ayf'(\eta), w = -\sqrt{va}f(\eta), \\ \text{and } \theta(\eta) = \frac{T - T_\infty}{T_0 - T_w}, \end{cases} \tag{6}$$

where  $\eta = \sqrt{\frac{a}{v}}z$  is a dimensionless variable,  $c$  is the distance between the axis of stagnation flow and the center of shrinking surface and  $b$  is shrinking rate and  $b < 0$  indicates the shrinking surface.

The equation of continuity (1) is satisfied. From equation (4), the pressure  $\pi$  is obtained as:

$$\pi = \pi_0 - \rho a^2 \frac{x^2}{2} - \rho a^2 \frac{y^2}{2} - \rho \frac{w^2}{2} + \rho v \frac{\partial w}{\partial z}.$$

The governing equations yield a set of non linear ordinary differential equations.

$$f''' + 1 = f'^2 - 2ff'', \tag{7}$$

$$g'' = gf' - 2g'f, \tag{8}$$

$$\theta'' + 2 \text{Pr} f \theta' = 0, \tag{9}$$

The boundary conditions are

$$\begin{cases} f = 0, f' = \alpha, g = 1, \theta = 1, & \text{at } \eta = 0, \\ f' \rightarrow 1, g \rightarrow 0, \theta \rightarrow 0, & \text{as } \eta \rightarrow \infty. \end{cases} \tag{10}$$

Where  $\alpha = \frac{b}{a}$ ,  $\text{Pr} = \frac{\rho \nu C_p}{K}$  and  $\nu = \frac{\mu}{\rho}$  is the coefficient of kinematic viscosity. The primes denote the differentiation with respect to  $\eta$ .

### 3 FINITE DIFFERENCE EQUATIONS

In order to obtain numerical solution of the equations (7) and (8) we put

$$P = f' \tag{11}$$

We get

$$P'' + 1 = P^2 - 2fP', \tag{12}$$

$$g'' = gP - 2g'f, \tag{13}$$

with the boundary conditions

$$\begin{cases} f = 0, P = \alpha, g = 1, \theta = 1, & \text{at } \eta = 0, \\ P \rightarrow 1, g \rightarrow 0, \theta \rightarrow 0, & \text{as } \eta \rightarrow \infty. \end{cases} \tag{14}$$

The equations (12), (13) and (9) by using central difference approximations at a typical point  $\eta = \eta_n$  of the interval  $[0, \infty)$  and the resulting finite difference equations are obtained below.

$$(4 + 2h^2 P_n) P_n = 2h^2 + (2 + 2hf_n) P_{n+1} + (2 - 2hf_n) P_{n-1}, \tag{15}$$

$$(4 + 2h^2 P_n) g_n = (2 + 2hf_n) g_{n+1} + (2 - 2hf_n) g_{n-1}, \tag{16}$$

$$2(\theta_{n+1} + \theta_{n-1}) + \text{Pr} f_n h (\theta_{n+1} - \theta_{n-1}) = 4\theta_n, \tag{17}$$

where  $h$  denotes the grid size and the symbols used denote  $f_n = f(\eta_n)$ ,  $P_n = P(\eta_n)$ ,  $g_n = g(\eta_n)$  and  $\theta_n = \theta(\eta_n)$ . For computational purposes, we replace the interval  $[0, \infty)$  by  $[0, \beta)$  where  $\beta$  is sufficiently large.

### 4 COMPUTATIONAL PROCEDURE

We now solve numerically the first order ordinary differential equation (11) and the system of finite difference equations (15) to (17) at each interior grid point of the interval. The equation (11) is integrated by the Simpson's (1/3) rule with the formula of Adams-Moulton, whereas the set of equations (15) to (17) are solved by using SOR iterative procedure subject to the appropriate conditions.

The order of the sequence of iterations is as follows:

1. The equations (15) to (17) are solved to calculate the values of  $P$ ,  $g$  and  $\theta$  subject to the boundary conditions

$$\begin{aligned} P = \alpha, \quad g = 1, \quad \theta = 1, & \quad \text{when } \eta = 0, \\ P = 1, \quad g = 0, \quad \theta = 0, & \quad \text{when } \eta \rightarrow \infty. \end{aligned}$$

2. The computed solutions of  $P$  are then employed into the equation (11) for the calculation of  $f$  with the condition:

$$f = 0 \quad \text{when } \eta = 0$$

3. In order to accelerate the speed of convergence of the SOR method, the optimum value of the relaxation parameter  $\omega_{opt}$  is estimated between 1 and 2. The optimum value of the relaxation parameter for the problem under consideration is 1.5.
4. The above procedure is repeated until convergence is obtained according to the criterion  $\max |U^{n+1} - U^n| < 10^{-6}$  where  $n$  denotes the number of iterations and  $U$  stands for each of the functional value.

For higher order accuracy, the above steps 1 to 4 are repeated for step sizes  $\frac{h}{2}$  and  $\frac{h}{4}$ .

## 5 DISCUSSION ON NUMERICAL RESULTS

The numerical computation has been performed for the values of parameter  $\alpha$  in the ranges  $-1.1 < \alpha \leq 10$ . The results have been calculated on three different grid sizes namely  $h=0.01, 0.005, 0.0025$ . The Table 1 to Table 5 contains the results for  $f, f', g$  and  $\theta$  for each of the above grid sizes. The results compare very well.

The values of functions  $f''(0)$  and  $g'(0)$  are obtained and compared with the previous results. The comparison is shown in Table 6 and presents a very good agreement with the results reported by Wang [1].

Figure 1 demonstrates the function  $f$  for non negative values of  $\alpha$ . The function  $f$  increases with the increasing values of  $\alpha$ . The function  $f$  has been plotted in Figure 2 for negative values of  $\alpha$ , the case for shrinking sheet. The function  $f$  is initially negative, for negative values of  $\alpha$ . When  $\alpha = 0$ ,  $f$  behaves like the axisymmetric stagnation flow towards a solid plate. The Figure 3 demonstrates the non-alignment function  $g$  for different values of parameter  $\alpha$ . The effect is larger for shrinking sheet but smaller in case of stretching sheet. The Figure 4 and Figure 5 depict respectively, the non-dimensional coefficient of skin friction  $f''(0)$  and the function  $g'(0)$ .

It is noticed that for increasing values of the shrinking parameter  $\alpha$ , the boundary layer thickness increase and hence the heat transfer rate decreases as shown in Figure 6. Also the heat transfer rate is not affected by the non-alignment function  $g$ .

## 6 CONCLUSION

The effects of different parameters are observed on the similarity, velocity and temperature profiles. The function  $f$  increases with the increasing values of  $\alpha$ . When  $\alpha = 0$ ,  $f$  behaves like the axisymmetric stagnation flow towards a solid plate. For increasing values of the shrinking parameter  $\alpha$ , the boundary layer thickness increase and hence the heat transfer rate decreases. The heat transfer rate is not affected by the non-alignment function  $g$ . The comparison is excellent with the results reported by Wang [1].

Table 1: The Numerical solutions of  $f, f', g$  and  $\theta$  for  $\alpha = -1.1$

$h$	$\eta$	$f$	$f'$	$g$	$\theta$
0.010	0.000	0.000000	-1.100000	1.000000	1.000000
	1.000	-1.339801	-1.573229	2.445890	0.999516
	2.000	-3.149518	-2.052835	3.642439	0.999324
	3.000	-5.464848	-2.589905	4.819904	0.999300
	4.000	-8.357139	-3.210315	6.064828	0.999378
	5.000	-11.710365	1.000000	0.000000	0.000000
0.005	0.000	0.000000	-1.100000	1.000000	1.000000
	1.000	-1.557032	-2.001907	3.116697	0.999974
	2.000	-3.995546	-2.875853	4.929018	0.999942
	3.000	-7.315375	-3.768956	6.658309	0.999869
	4.000	-11.546136	-4.699814	8.375803	0.999834
	5.000	-16.524296	1.000000	0.000000	0.000000
0.0025	0.000	0.000000	-1.100000	1.000000	1.000000
	1.000	-1.612966	-2.110356	4.354181	0.999844
	2.000	-4.205258	-3.071135	7.291046	0.999170
	3.000	-7.753620	-4.026309	10.036325	0.998049
	4.000	-12.261209	-4.991234	12.665633	0.997116
	5.000	-17.539229	1.000000	0.000000	0.000000

Table 2: The Numerical solutions of  $f, f', g$  and  $\theta$  for  $\alpha = -0.5$

$h$	$\eta$	$f$	$f'$	$g$	$\theta$
0.010	0.000	0.000000	-0.500000	1.000000	1.000000
	1.000	0.116551	0.600363	0.385642	0.514382
	2.000	0.946768	0.962018	0.048265	0.126728
	3.000	1.936048	0.999392	0.001282	0.010375
	4.000	2.936079	1.000132	0.000006	0.000241
	5.000	3.936144	1.000000	0.000000	0.000000
0.005	0.000	0.000000	-0.500000	1.000000	1.000000
	1.000	0.116820	0.600880	0.149585	0.211803
	2.000	0.947450	0.962219	0.004013	0.009718
	3.000	1.936741	0.999224	0.000020	0.000103
	4.000	2.936606	0.999989	0.000000	0.000000
	5.000	3.936568	1.000000	0.000000	0.000000
0.0025	0.000	0.000000	-0.500000	1.000000	1.000000
	1.000	0.116889	0.601068	0.004490	0.010450
	2.000	0.947676	0.962299	0.000000	0.000000
	3.000	1.936989	0.999224	0.000000	0.000000
	4.000	2.936856	0.999993	0.000000	0.000000
	5.000	3.936822	1.000000	0.000000	0.000000

Table 3: The Numerical solutions of  $f, f', g$  and  $\theta$  for  $\alpha = 0.0$

$h$	$\eta$	$f$	$f'$	$g$	$\theta$
0.010	0.000	0.000000	0.000000	1.000000	1.000000
	1.000	0.492445	0.829932	0.233433	0.374884
	2.000	1.433171	0.992047	0.014111	0.055081
	3.000	2.431450	1.000135	0.000158	0.002448
	4.000	3.431604	1.000118	0.000000	0.000030
0.005	0.000	0.000000	0.000000	1.000000	1.000000
	1.000	0.492583	0.830109	0.162127	0.224374
	2.000	1.433367	0.991935	0.005751	0.015200
	3.000	2.431339	0.999784	0.000038	0.000286
	4.000	3.431176	0.999875	0.000000	0.000002
0.0025	0.000	0.000000	0.000000	1.000000	1.000000
	1.000	0.492664	0.830248	0.006277	0.015968
	2.000	1.433527	0.991956	0.000000	0.000002
	3.000	2.431509	0.999790	0.000000	0.000000
	4.000	3.431354	0.999880	0.000000	0.000000
0.0025	0.000	0.000000	0.000000	1.000000	1.000000
	1.000	0.492664	0.830248	0.006277	0.015968
	2.000	1.433527	0.991956	0.000000	0.000002
	3.000	2.431509	0.999790	0.000000	0.000000
	4.000	3.431354	0.999880	0.000000	0.000000
0.0025	0.000	0.000000	0.000000	1.000000	1.000000
	1.000	0.492664	0.830248	0.006277	0.015968
	2.000	1.433527	0.991956	0.000000	0.000002
	3.000	2.431509	0.999790	0.000000	0.000000
	4.000	3.431354	0.999880	0.000000	0.000000
0.0025	0.000	0.000000	0.000000	1.000000	1.000000
	1.000	0.492664	0.830248	0.006277	0.015968
	2.000	1.433527	0.991956	0.000000	0.000002
	3.000	2.431509	0.999790	0.000000	0.000000
	4.000	3.431354	0.999880	0.000000	0.000000
0.0025	0.000	0.000000	0.000000	1.000000	1.000000
	1.000	0.492664	0.830248	0.006277	0.015968
	2.000	1.433527	0.991956	0.000000	0.000002
	3.000	2.431509	0.999790	0.000000	0.000000
	4.000	3.431354	0.999880	0.000000	0.000000
0.0025	0.000	0.000000	0.000000	1.000000	1.000000
	1.000	0.492664	0.830248	0.006277	0.015968
	2.000	1.433527	0.991956	0.000000	0.000002
	3.000	2.431509	0.999790	0.000000	0.000000
	4.000	3.431354	0.999880	0.000000	0.000000
0.0025	0.000	0.000000	0.000000	1.000000	1.000000
	1.000	0.492664	0.830248	0.006277	0.015968
	2.000	1.433527	0.991956	0.000000	0.000002
	3.000	2.431509	0.999790	0.000000	0.000000
	4.000	3.431354	0.999880	0.000000	0.000000

Table 4: The Numerical solutions of  $f, f', g$  and  $\theta$  for  $\alpha = 5.0$

$h$	$\eta$	$f$	$f'$	$g$	$\theta$
0.010	0.000	0.000000	5.000000	1.000000	1.000000
	1.000	2.117306	1.069530	0.020969	0.073819
	2.000	3.130389	1.000280	0.000066	0.001339
	3.000	4.130564	1.000162	0.000000	0.000006
	4.000	5.130687	1.000083	0.000000	0.000000
0.005	0.000	0.000000	5.000000	1.000000	1.000000
	1.000	2.117190	1.069490	0.013487	0.035595
	2.000	3.130239	1.000166	0.000017	0.000169
	3.000	4.130232	0.999947	0.000000	0.000000
	4.000	5.130149	0.999922	0.000000	0.000000
0.0025	0.000	0.000000	5.000000	1.000000	1.000000
	1.000	2.116875	1.069412	0.000105	0.000527
	2.000	3.129937	1.000222	0.000000	0.000000
	3.000	4.129982	0.999978	0.000000	0.000000
	4.000	5.129913	0.999959	0.000000	0.000000
0.0025	0.000	0.000000	5.000000	1.000000	1.000000
	1.000	2.116875	1.069412	0.000105	0.000527
	2.000	3.129937	1.000222	0.000000	0.000000
	3.000	4.129982	0.999978	0.000000	0.000000
	4.000	5.129913	0.999959	0.000000	0.000000
0.0025	0.000	0.000000	5.000000	1.000000	1.000000
	1.000	2.116875	1.069412	0.000105	0.000527
	2.000	3.129937	1.000222	0.000000	0.000000
	3.000	4.129982	0.999978	0.000000	0.000000
	4.000	5.129913	0.999959	0.000000	0.000000
0.0025	0.000	0.000000	5.000000	1.000000	1.000000
	1.000	2.116875	1.069412	0.000105	0.000527
	2.000	3.129937	1.000222	0.000000	0.000000
	3.000	4.129982	0.999978	0.000000	0.000000
	4.000	5.129913	0.999959	0.000000	0.000000
0.0025	0.000	0.000000	5.000000	1.000000	1.000000
	1.000	2.116875	1.069412	0.000105	0.000527
	2.000	3.129937	1.000222	0.000000	0.000000
	3.000	4.129982	0.999978	0.000000	0.000000
	4.000	5.129913	0.999959	0.000000	0.000000

Table 5: The Numerical solutions of  $f, f', g$  and  $\theta$  for  $\alpha = 10.0$

$h$	$\eta$	$f$	$f'$	$g$	$\theta$
0.010	0.000	0.000000	10.000000	1.000000	1.000000
	1.000	2.933625	1.040116	0.005179	0.028013
	2.000	3.939659	1.000164	0.000004	0.000174
	3.000	4.939822	1.000145	0.000000	0.000000
	4.000	5.939930	1.000074	0.000000	0.000000
0.005	0.000	0.000000	10.000000	1.000000	1.000000
	1.000	2.933690	1.040124	0.003937	0.015535
	2.000	3.939662	1.000000	0.000001	0.000030
	3.000	4.939633	0.999941	0.000000	0.000000
	4.000	5.939561	0.999929	0.000000	0.000000
0.0025	0.000	0.000000	10.000000	1.000000	1.000000
	1.000	2.933167	1.040061	0.000067	0.000360
	2.000	3.939211	1.000119	0.000000	0.000000
	3.000	4.939284	1.000016	0.000000	0.000000
	4.000	5.939307	1.000008	0.000000	0.000000
5.000	6.939339	1.000000	0.000000	0.000000	

Table 6: The comparison of present results for  $f''(0)$  and  $g'(0)$  with the Wang results

$\alpha$	$f''(0)$		$g'(0)$	
	Present Results	Results of Wang[1]	Present Results	Results of Wang[1]
0	1.3122251	1.311938	-0.9386957	-0.93873
0.1	1.2292832	1.22911	-1.0035276	-1.0040
0.2	1.1339485	1.13374	-1.0649502	-1.0659
0.5	0.7805824	0.78032	-1.2329936	-1.2355
1.0	-0.9536	0	-1.4740705	-1.4793
2.0	-2.126980	-2.13107	-1.8699347	-1.8800
5.0	-11.776734	-11.8022	-2.736712	-2.7617
8.0	-25.026512	-----	-3.387072	-----
10.0	-35.45265	-----	-3.757072	-----
-0.05	1.3486698	-----	-0.9048998	-----
-0.15	1.4107167	-----	-0.8338392	-----
-0.25	1.4570951	1.45664	-0.7576227	-0.75639
-0.5	1.4901995	1.49001	-0.5349279	-0.53237
-0.75	1.3530015	1.35284	-0.2245247	-0.22079
-0.95	0.9458780	0.94690	0.2645135	0.26845
-0.9945	0.6551266	0.5	0.6122589	0.83183
-1.10	-1.0703086	-----	1.7551898	-----

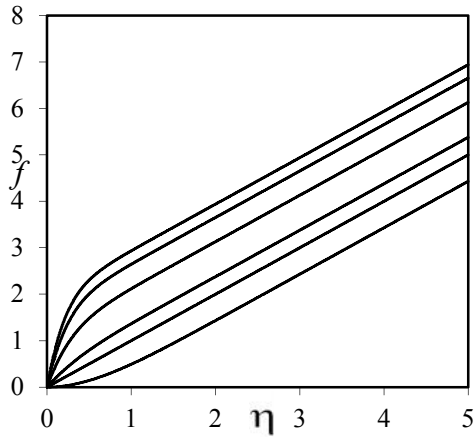


Figure 1: Graph of function  $f$  for  $\alpha = 0, 1, 2, 5, 8$  and  $10$  from bottom

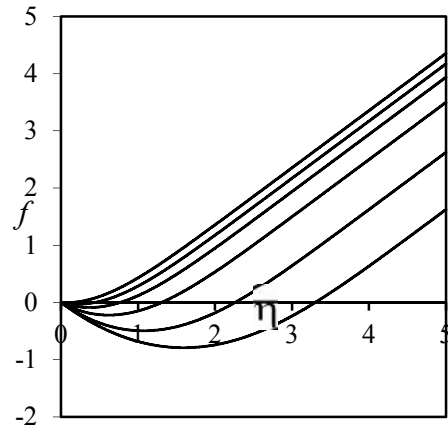


Figure 2: Graph of function  $f$  for  $\alpha = -0.1, -0.3, -0.5, -0.75, -0.95$  and  $-1$  from top

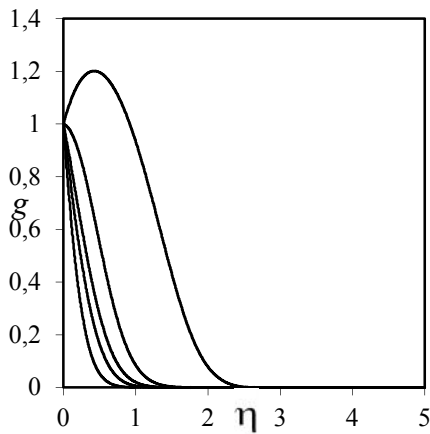


Figure 3: Graph of function  $g$  for  $\alpha = 1, 0, -0.5, -0.75, -0.95$  and  $-1.0$  from bottom.

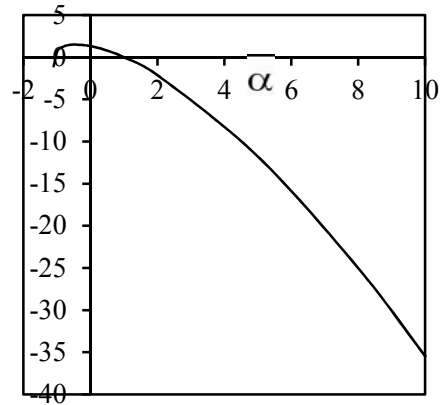


Figure 4: Graph of the skin friction coefficient  $f''(0)$  against  $\alpha$

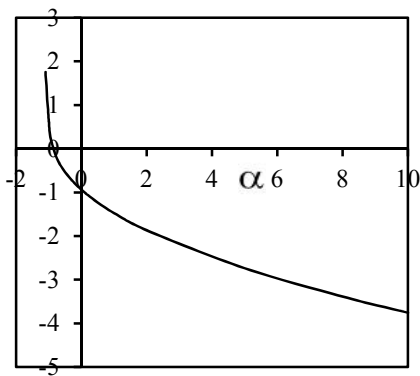


Figure 5: Graph of the gradient of non alignment function  $g$  i.e.  $g'(0)$

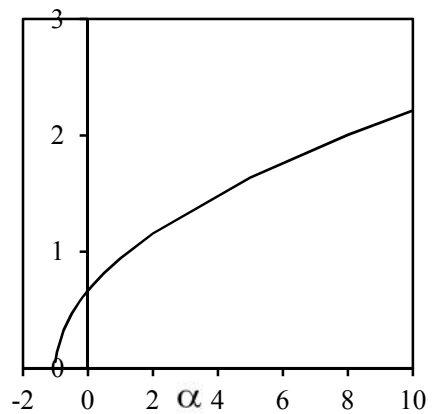


Figure 6: Graph of  $-\theta'(0)$  for different values of  $\alpha$  when  $Pr=0.7$

## REFERENCES

- [1] Wang, C.Y., Stagnation flow towards a shrinking sheet, *International Journal of Non-Linear Mechanics*, 43, 377 – 382, 2008.
- [2] Fang, T. and Zhang, Ji., Closed- Form exact solutions of MHD viscous flow over a shrinking sheet, *Commun Nonlinear Sci Numer Simulat*, 14, 2853 –2857, 2009.
- [3] T. Hayat, Z. Abbas and M. Sajid, On the Analytic Solution of MHD Flow of a Second Grade Fluid Over a Shrinking Sheet, *J. Appl. Mech.* 74(6), pp1165- 1171, 2007.
- [4] Tiegang Fang, Boundary layer flow over a shrinking sheet with power-law velocity, *International Journal of Heat and Mass Transfer*, Volume 51, Issues 25–26, 5838–5843, 2008.
- [5] S. Nadeem, Rizwan Ul Haq, C. Lee, MHD flow of a Casson fluid over an exponentially shrinking sheet, *Scientia Iranica B* 19 (6), 1550–1553, 2012.
- [6] A. Ara, N. Alam Khan, Hassam Khan, Faqiha Sultan, Radiation effect on boundary layer flow of an Eyring–Powell fluid over an exponentially shrinking sheet, *Ain Shams Engineering Journal*, Volume 5, Issue 4, 1337–1342, 2014.
- [7] Khairy Zaimi, Anuar Ishak, Ioan Pop, Boundary layer flow and heat transfer over a nonlinearly permeable stretching/shrinking sheet in a nanofluid, *Scientific Reports* 4, Article number:4404 doi:10.1038/ srep04404, 2014.
- [8] Khairy Zaimi,, Anuar Ishak, Ioan Pop, Flow Past a Permeable Stretching/Shrinking Sheet in a Nanofluid Using Two-Phase Model, *PLoS ONE* 9(11): e111743, 2014.
- [9] Sajid, M. and Hayat, T., The application of homotopy analysis method for MHD viscous flow due to a shrinking sheet, *Chaos Soliton Fractals*, 39, 1317-1323, 2009.
- [10] Noor, N. F. M., Kechil, S. A. and Hashim, I., Simple non-perturbative solution for MHD viscous flow due to a shrinking sheet, *Commun Nonlinear Sci Numer Simulat* 15, 144-148, 2010.
- [11] C. F. Gerald, "Applied Numerical Analysis," Addison- Wesley Publication, New York, 1989.